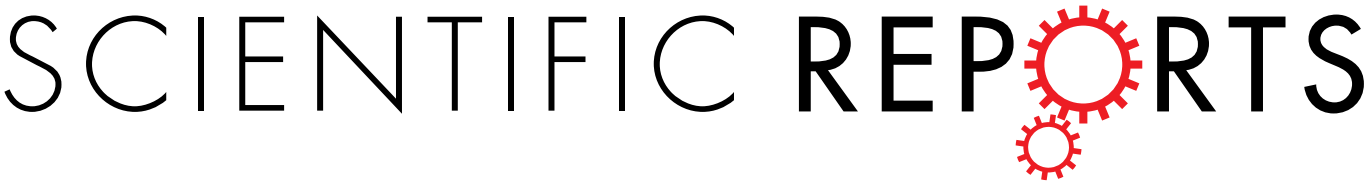

OPEN

Disorder and defects are not intrinsic to boron carbide

Swastik Mondal[1,2], Elena Bykova[2,3], Somnath Dey[2], Sk Imran Ali[2,†], Natalia Dubrovinskaia[2], Leonid Dubrovinsky[3], Gleb Parakhonskiy[2,3] & Sander van Smaalen[2]

Received: 21 August 2015
Accepted: 11 December 2015
Published: 18 January 2016

A unique combination of useful properties in boron-carbide, such as extreme hardness, excellent fracture toughness, a low density, a high melting point, thermoelectricity, semi-conducting behavior, catalytic activity and a remarkably good chemical stability, makes it an ideal material for a wide range of technological applications. Explaining these properties in terms of chemical bonding has remained a major challenge in boron chemistry. Here we report the synthesis of fully ordered, stoichiometric boron-carbide $B_{13}C_2$ by high-pressure–high-temperature techniques. Our experimental electron-density study using high-resolution single-crystal synchrotron X-ray diffraction data conclusively demonstrates that disorder and defects are not intrinsic to boron carbide, contrary to what was hitherto supposed. A detailed analysis of the electron density distribution reveals charge transfer between structural units in $B_{13}C_2$ and a new type of electron-deficient bond with formally unpaired electrons on the C–B–C group in $B_{13}C_2$. Unprecedented bonding features contribute to the fundamental chemistry and materials science of boron compounds that is of great interest for understanding structure-property relationships and development of novel functional materials.

Boron carbide is one of the hardest substances, surpassed only by diamond and boron nitride[1]. The high mechanical and thermal stability, low density and low costs of fabrication have made boron carbide the prime choice in a series of technological applications[1–7]. Boron carbide preserves the same structure for a range of compositions, and details of this crystal structure have been discussed in terms of chemical disorder of boron and carbon atoms as well as the presence of vacancies[1,8–11]. Electronic-structure calculations suggest that the properties of boron carbide depend on the stoichiometry and the details of the disorder[2,7,12,13].

Experimentally, chemical bonding can be accessed through single-crystal x-ray diffraction. Reliable information on the distribution of the electron density in the unit cell can be obtained only for good-quality single crystals with minimal structural disorder[14]. Synthesis of defect-free material is the most challenging task in boron carbide chemistry. We have succeeded in growing small single crystals of the stoichiometric composition $B_{13}C_2$ by high-pressure–high-temperature techniques (see *Methods*). The material is transparent with a dark red or maroon color, indicating an insulator or a large-band-gap semiconductor. This is in agreement with some literature data[15], but it is inconsistent with the relatively high electrical conductivity reported for boron carbide[1]. To the best or our knowledge, dark red transparent boron carbide has not been reported before.

A multipole (MP) model has been obtained for the crystal structure of $B_{13}C_2$ by refinement against accurately measured intensities of Bragg reflections (see *Methods* and Supplementary Information Section S1)[14]. The excellent fit to the diffraction data with $R_1 = 0.0197$ provides strong evidence for the stoichiometry of $B_{13}C_2$, in agreement with the composition obtained by Energy-dispersive x-ray (EDX) analysis (see *Methods*). The excellent fit furthermore indicates the absence of disorder: $B_{13}C_2$ is composed of B_{12} icosahedral clusters and CBC linear chains (Fig. 1 and Supplementary Information Section S2). Lattice parameters and values of atomic displacement parameters (ADPs) fall within a range previously assigned to the composition $B_{12}C_3$[1,8–10]. The possibility of different compositions was investigated by additional MP refinements with small amounts of carbon at the B_P site, corresponding to $B_{12+x}C_{3-x}$ stoichiometries with $x = 0.44$ and $x = -0.11$, respectively (see Supplementary Information Section S1 for details). Both models gave a slightly worse fit to the diffraction data than the $B_{13}C_2$ model. More importantly, the number of valence electrons of C at the B_P site refined to zero, thus showing that the MP refinement has effectively removed carbon from the B_P site, providing further support for the ordered

[1]Max-Planck-Institut fuer Kohlenforschung, Kaiser-Wilhelm-Platz 1, 45470 Muelheim an der Ruhr, Germany. [2]Laboratory of Crystallography, University of Bayreuth, D-95440 Bayreuth, Germany. [3]Bayerisches Geoinstitut, University of Bayreuth, D-95440 Bayreuth, Germany. [†]Present address: Department of Materials and Environmental Chemistry, Stockholm University, SE-10691 Stockholm, Sweden. Correspondence and requests for materials should be addressed to S.M. (email: mondal@mpi-muelheim.mpg.de) or S.v.S. (email: smash@uni-bayreuth.de)

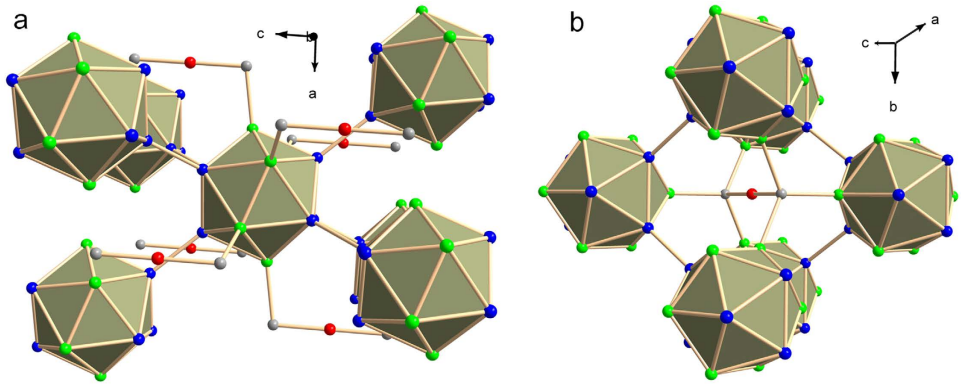

Figure 1. Crystal structure of $B_{13}C_2$. (**a**) Perspective view highlighting the environment of the icosahedral B_{12} cluster. Each B_{12} cluster is bonded by B_P–B_P bonds to three B_{12} clusters in each of the two neighboring close-packed planes, and to six CBC chains by C–B_E bonds. (**b**) Perspective view highlighting the environment of the CBC chain. Each carbon atom is bonded to three B_{12} clusters within a single close-packed plane. Color code: B_P is blue, B_E is green, B_C is red, and C is grey.

stoichiometric character of the investigated crystal. Interestingly, a refinement of the independent atom model (IAM) including the site occupancy factors of C at the B_P and B_E sites resulted in 19% occupancy of the B_P site by carbon ($x = -0.11$). Contrary to the MP model ($R_1 = 0.0197$), the IAM with disorder ($R_1 = 0.0287$) leads to only a small improvement of the fit to the data (Table S4). These results suggest that the charge transfer towards B_P in the MP model is mimicked in the disordered IAM by a fractional occupancy of the B_P site by C.

Discrepancies between the present values of the lattice parameters and ADPs and those reported in the literature[1,8–10] for the same composition may be the result of different degrees of disorder and defects between different samples. The single MP refinement[16] reported previously for $B_{13}C_2$ gave a much worse fit to their XRD data ($R_1 = 0.0440$), which questions the reliability of that model. The single MP refinement[17] for $B_{12}C_3$ also led to a substantially worse fit to their XRD data ($R_1 = 0.0250$) than we have obtained for our model against the present XRD data ($R_1 = 0.0197$). Thus, a highly precise MP refinement refutes recent less accurate diffraction studies[13] and theoretical electronic-structure calculations[2,12], where a disorderly replacement by carbon of a certain fraction of the boron atoms of the B_{12} clusters was considered as absolutely essential for the stability of $B_{13}C_2$.

The MP model extends the independent atom model (IAM) of spherical atoms by parameters describing the reorganization of electron density due to chemical bonding. Previous electron-density studies on boron carbide[18,19] have been restricted to a discussion of the qualitative features of the electron densities. Quantitative information about chemical bonding can be extracted from the static electron density of the MP model through its topological properties according to Bader's *quantum theory of atoms in molecules* (QTAIM)[14,20]. Critical points (CPs) are defined as the positions where the gradient of the electron density is zero [$\nabla\rho(\mathbf{r}) = 0$][20]. They are classified according to the number of positive eigenvalues of the Hessian matrix of second derivatives as local maxima (3 positive eigenvalues), bond critical points BCPs (2), ring critical points RCPs (1) and local minima (0 positive eigenvalues)[20].

All atomic positions of the present MP model can be identified with local maxima in the static electron density, while additional local maxima do not exist. BCPs and RCPs have been found between the atoms of the B_{12} cluster in a similar pattern as for α-boron[21], and with comparable values for the electron densities and Laplacians (Table 1). Together, these features indicate similar bonding by molecular-type orbitals on the B_{12} clusters in $B_{13}C_2$ and α-boron[21]. According to Wade's rule[22], this bonding involves 26 of the 36 valence electrons of the twelve boron atoms of this closo-cluster, thus leaving for each boron atom one orbital but only 5/6 electrons for exo-cluster bonding[21,23].

The crystal structure of $B_{13}C_2$ comprises four crystallographically independent atoms. CBC chains contain the carbon atom and a boron atom denoted as B_C; the B_{12} cluster is made of six polar and six equatorial atoms, denoted as B_P and B_E, respectively (Fig. 1). According to the QTAIM[20], bonding between a pair of atoms exists, if the electron density possesses a BCP between those atoms. For $B_{13}C_2$, we have found BCPs between pairs of B_P atoms from neighboring clusters. The distance B_P–B_P is slightly larger and the magnitudes of the electron density, ρ_{BCP}, and Laplacian, $\nabla^2\rho_{BCP}$, are slightly smaller than those of the corresponding inter-cluster bonds in α-boron[21] and γ-boron[24] (Table 1). The high value of ρ_{BCP} together with a negative value of $\nabla^2\rho_{BCP}$ of large magnitude indicate a strong covalent interaction between these atoms[20]. The similarities with bonding in α-boron[21] (Table 1) allow this bond to be classified as a 2-electron-2-center (2e2c) bond. Further evidence for this interpretation comes from the QTAIM theory, which assigns a charge to each atom by integration of the electron density over the atomic basins. A charge of -0.21 electrons has been obtained by integrating the experimental static electron density over the atomic basin of B_P (Table 2). This value is in good agreement with electron counting. With 5/6 electrons per boron atom available for exo-cluster bonding, a formal charge of -0.17 is obtained for B_P involved in a 2e2c B_P–B_P exo-cluster bond.

Bond-critical points are also found between a B_E atom and the closest C atom. Large magnitudes of ρ_{BCP} and the negative Laplacian $\nabla^2\rho_{BCP}$ indicate a strong covalent interaction and a 2e2c C–B_E bond. An equal split of these

Bond	d (Å)	d_{BCP} (Å)	ρ_{BCP} (e/Å^3)	$\nabla^2\rho_{BCP}$ (e/Å^5)
Bonds in $B_{13}C_2$				
C–B_E	1.6037(2)	1.082/0.523	1.097	−8.289
C–B_C	1.4324(5)	0.938/0.494	1.556	−8.985
B_P–B_P	1.7131(4)	0.857/0.857	1.030	−6.463
Inter-cluster bonds in α-boron				
B1–B1 (*2e2c*)[21]	1.6734(3)	0.837/0.837	1.104	−9.572
Inter-cluster bonds in γ-boron				
B3–B3 (*2e2c*)[24]	1.6599(5)	0.830/0.830	1.165	−10.404
B1–B4 (*1e2c*)[24]	1.8275(2)	0.865/0.979	0.782	−4.002

Table 1. Geometries and topological properties of the experimental static electron density for 2-center *exo*-cluster bonds in $B_{13}C_2$. d is the bond-length and d_{BCP} is the distance between a BCP and each of the two constituent atoms of that bond. ρ_{BCP} is the electron density at the BCP and $\nabla^2\rho_{BCP}$ is its Laplacian. Topological properties for the inter-cluster B–B bonds in α-boron[21] and in γ-boron[24] are also given.

Atom	Multiplicity	V_{Basin} (Å^3)	Charge (e)
B_P	6	7.808	−0.210
B_E	6	5.176	+0.703
C	2	14.571	−2.610
B_C	1	1.936	+2.298

Table 2. Atomic basins (volume V_{Basin}) and ionic charges for the four crystallographically independent atoms in $B_{13}C_2$ along with their multiplicity in the unit cell.

electrons between C and B_E again gives a formal charge of −0.17 for B_E, and it would result in a $(B_{12})^{2-}$ group[2] However, carbon is more electronegative than boron and should attract most of the bonding electrons. Indeed, the integration of the electron density over the atomic basins leads to a positive atom B_E and a strongly negative C atom (Table 2). A detailed analysis of the electron density shows that the positive charge of B_E is the result of a strong polar-covalent character of the C–B_E bond, with the BCP much closer to B_E than to C (Fig. 2; Table 1), but with a large value of ρ_{BCP} as opposed to an expected small value for ionic bonding[20].

With the interpretation of B_P–B_P and C–B_E bonds as 2e2c bonds, only three electrons are left for the two C–B_C bonds of the CBC group (see Supplementary Material Section S3). These bonds can therefore be described as a three-electron-three-center (3e3c) bond or as resonance between two equivalent combinations of one 2e2c and one 1e2c bond (Fig. 3). The large values of the electron density along the bond path (Fig. 2a) correlate with the short bond length, which is explained by the internal pressure on the CBC group[2]. Large magnitudes of ρ_{BCP} and $\nabla^2\rho_{BCP}$ indicate a covalent interaction. The electron deficient character of this bond is in complete agreement with the ionic charge of +2.30 of B_C. The latter value is the result of the extremely small volume of the atomic basin of this atom, which demonstrates that the internal pressure has squeezed out most of the electrons of B_C, reminiscent of the effect of pressure on the electrons in lithium metal[25].

A 3e3c C–B_C–C bond contains one unpaired electron per formula unit $B_{13}C_2$. Experimentally, unpaired spins have been observed at much lower concentrations in boron carbides of different compositions[2,4,5,26,27]. One explanation lies in chemical disorder and vacancies, which are necessarily present for other compositions than stoichiometric $B_{13}C_2$, and which reduce the number of unpaired spins. On the other hand, the itinerant character of the electron states or localization as bipolarons may be in agreement with low concentrations of unpaired spins[2,5,12]. The presence of an unsaturated bond on the CBC chains should result in a high chemical reactivity of this bond. However, we have found that B_C is extremely small (Table 2) and well shielded from the outside by C atoms and bulky B_{12} clusters. Steric effects hindering access to reactive sites is known to stabilize radicals[28,29]. High temperatures can overcome these barriers, and a high reactivity at elevated temperatures towards oxidizing agents has been described for boron carbide[30]. Recently, amorphisation[6,31] of boron carbide $B_{12}C_3$ has been explained on the basis of the presence of carbon atoms at a small fraction of the B_P sites[32]. Stoichiometric $B_{13}C_2$ is a form of boron carbide that lacks this detrimental property of technical boron carbide with compositions on the carbon-rich side of $B_{13}C_2$.

In summary, we have synthesized stoichiometric boron carbide $B_{13}C_2$, which is free of intrinsic disorder, and is built of B_{12} icosahedral clusters and C–B_C–C chains. Unlike band-structure calculations[2,12] on fully ordered $B_{13}C_2$, the ordered stoichiometric compound is an insulator or large band-gap semiconductor. An experimental electron-density study by X-ray diffraction conclusively determines that $B_{13}C_2$ is an electron-precise material. The electron-deficient character is explained by B_C being stripped of two of its valence electrons and the existence of a unique, electron deficient 3e3c bond on the C–B_C–C chains. The low chemical reactivity follows from the extremely small volume of B_C.

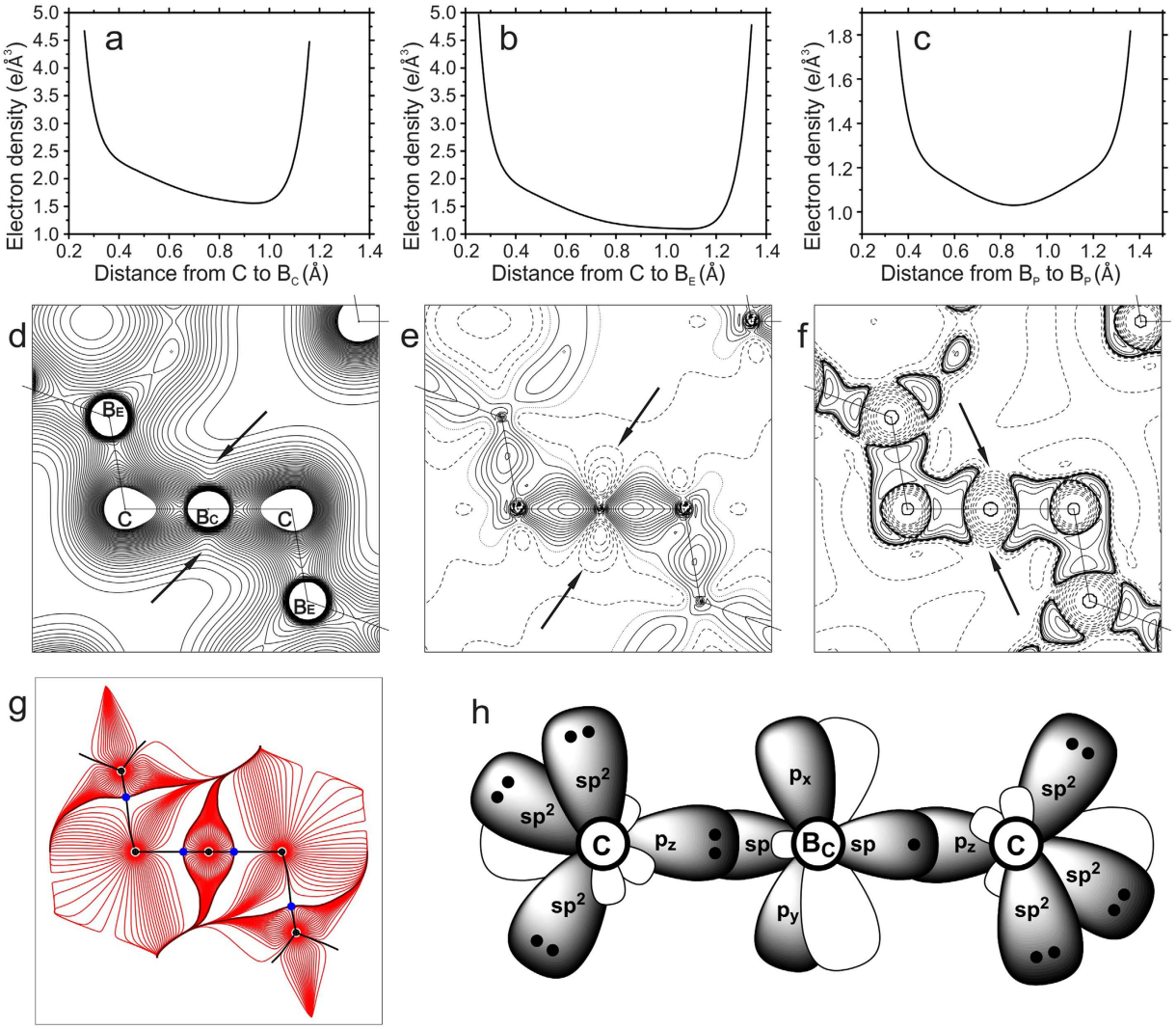

Figure 2. ED distribution in *exo*-cluster bonds and orbital hybridization scheme. (**a**) Electron density along the C–B_C bond path. (**b**) ED along the C–B_E bond path. (**c**) ED along the inter-cluster B_P–B_P bond path. (**d**) ED distribution in the B_E–C–B_C plane. Contour lines are at 0.05 eÅ^{-3} up to 2.00 eÅ^{-3}. A groove-like feature in the ED around the B_C atom (indicated by arrows) suggests the absence of electrons. (**e**) Dynamic deformation density map[18] in the same plane. Contour lines are at 0.05 eÅ^{-3} intervals; positive, negative and zero contours are drawn as solid, dashed and dotted lines respectively. Negative ED contours in the region shown by the arrows indicate empty 2p orbitals of B_C. (**f**) Laplacian in the same plane showing the valence shell charge concentrations (VSCC) around each atom. Contour lines at $\pm(2, 4, 8) \times 10^n$ eÅ^{-5} ($-3 \leq n \leq 3$). No VSCC has been found in the regions indicated by arrows, again pointing to empty 2p orbitals of B_C. (**g**) Gradient trajectories of the ED with BCPs (blue dots) indicated. It can be noticed that the volume of the B_C atomic basin is small and trajectories inside the basin are squeezed along the direction perpendicular to CBC chain indicating depletion of electrons. (**h**) The orbital hybridization scheme for C and B_C atoms. Filled orbitals are indicated by black dots representing electrons. The orbitals p_x and p_y of the atom B_C are empty.

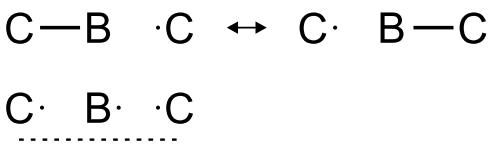

Figure 3. Resonance representation of the 3e3c bond on CBC chains.

Methods summary

Crystal growth. Single crystals of boron-carbide were grown at high pressures of 8.5–9 GPa and high temperatures of 1873–2073 K using a 1200-ton (Sumitomo) multi-anvil hydraulic press at the Bayerisches

Geoinstitut. Energy-dispersive x-ray (EDX) analysis has been employed to determine the composition as $B_{6.51(12)}C$, in agreement with stoichiometric $B_{13}C_2$. The presence of other elements could be excluded.

X-ray diffraction experiment for/and electron density analysis. A single crystal of boron-carbide of dimensions $0.09 \times 0.08 \times 0.05$ mm^3 was chosen for an x-ray diffraction experiment with synchrotron radiation at beamline F1 of Hasylab, DESY in Hamburg, Germany. The sample was kept at a temperature of 100 K, while a complete data set of accurate intensities was measured for Bragg reflections up to $\sin(\theta)/\lambda = 1.116$ Å^{-1}. The diffraction data were integrated using the computer program EVAL[33]. Structure refinements have been performed with the software XD2006[34]. A topological analysis of the static electron density has been performed by the modules TOPXD and XDPROP of the computer program XD2006. Two-dimensional density maps have been generated by the module XDGRAPH. See the Supplementary Information for details on procedures and the MP model.

References

1. Domnich, V., Reynaud, S., Richard, A., Haber, R. A. & Chhowalla, M. Boron Carbide: Structure, Properties, and Stability under Stress. *J. Amer. Ceram. Soc.* **94,** 3605–3628 (2011).
2. Balakrishnarajan, M. M., Pancharatna, P. D. & Hoffmann, R. Structure and bonding in boron carbide: The invincibility of imperfections. *New. J. Chem.* **31,** 473–485 (2007).
3. Thevenot, F. Boron carbide — a comprehensive review. *J. Eur. Ceram. Soc.* **6,** 205–225 (1990).
4. Kakazey, M. G., Gonzalez-Rodriguez, J. G., Vlasova, M. V. & Shanina, B. D. Electron paramagnetic resonance in boron carbide. *J. Appl. Phys.* **91,** 4438–4446 (2002).
5. Aselage, T. L., Emin, D. & McCready, S. S. Conductivities and Seebeck coefficients of boron carbides: Softening bipolaron hopping. *Phys. Rev. B* **64,** 054302 (2001)
6. Chen, M., McCauley, J. W. & Hemker, K. J. Shock-induced localized amorphization in boron carbide. *Science* **299,** 1563–1566 (2003).
7. Liu, J. *et al.* Boron carbides as efficient, metal-free, visible-light-responsive photocatalysts. *Angew. Chem. Int. Ed.* **52,** 3241–3245 (2013).
8. Morosin, B., Mullendore, A. W., Emin, D. & Slack, G. A. Rhombohedral crystal structure of compounds containing boron-rich icosahedra. Paper presented at the conference on Boron-Rich Solids, Albuquergue, USA (29–31 July 1985). Paper published in Boron-Rich Solids, Edited by Emin, D., Aselage, T., Beckel, C. L., Howard, I. A. & Wood, C. *AIP Conf. Proc.* **140**, 70–86 (1986), doi: 10.1063/1.35589.
9. Aselage, T. L. & Emin, D. Structural model of the boron carbide solid solution. Paper presented at the Tenth International Symposium on Boron, Borides, and Related Compounds, Albuquerque, USA (1990). Paper published in Boron Rich Solids, edited by Emin, D., Aselage, T. L., Switendick, A. C., Morosin, B. & Beckel, C. L. *AIP Conf. Proc.* **231**, 177–185 (1991). doi: 10.1063/1.40890.
10. Kwei, G. H. & Morosin, B. Structures of the Boron-Rich Boron Carbides from Neutron Powder Diffraction: Implications for the Nature of the Inter-Icosahedral Chains. *J. Phys. Chem.* **100,** 8031–8039 (1996).
11. Werheit, H. & Shalamberidze, S. Advanced microstructure of boron carbide. *J. Phys.: Condens. Matter* **24,** 385406 (2012).
12. Shirai, K., Sakuma, K. & Uemura, N. Theoretical study of the structure of boron carbide $B_{13}C_2$. *Phys. Rev. B* **90,** 064109 (2014).
13. Dera, P., Manghnani, M. H., Hushur, A., Hu, Y. & Tkachev, S. S. New insights into the enigma of boron carbide inverse molecular behavior. *J. Sol. State Chem.* **215,** 85–93 (2014).
14. Gatti, C. & Macchi, P. (Eds.) *Modern charge-density analysis*. Springer, Dordrecht (2012).
15. Werheit, H. & Gerlach, G. Dynamical conductivity of boron carbide: heavily damped plasma vibrations. *J. Phys.: Condens. Matter* **26,** 425801 (2014).
16. Kirfel, A., Gupta, A. & Will, G. The nature of the chemical bonding in boron carbide, $B_{13}C_2$. I. Structure refinement. *Acta Crystallogr. Sect. B* **35,** 1052–1059 (1979).
17. Baldinozzi, G., Dutheil, M., Simeone, D. & Leithe-Jasper, A. Charge density in disordered boron carbide: B12C3. An experimental and ab-initio study. Paper presented at the Materials Research Society Spring Meeting - Symposium V – Materials for Energy Storage, Generation, and Transport, San Francisco, USA (2002). *Mater. Res. Soc. Symp. Proc.* **730,** V.7.4.1–V.7.4.6 (2002). doi: 10.1557/PROC-730-V7.4
18. Kirfel, A., Gupta, A. & Will, G. The nature of the chemical bonding in boron carbide, $B_{13}C_2$. II. Dynamic deformation densities and valence densities. *Acta Crystallogr. Sect. B* **35,** 2291–2300 (1979).
19. Hosoi, S. *et al.* Electron density distributions in derivative crystals of α-rhombohedral boron. *J. Phys. Soc. Jpn.* **76,** 044602 (2007).
20. Bader, R. F. W. *Atoms in Molecules - a Quantum Theory*, Oxford University Press, Oxford, UK (1990).
21. Mondal, S. *et al.* Experimental evidence of orbital order in α-B_{12} and γ-B_{28} polymorphs of elemental boron. *Physical Review B* **88,** 024118 (2013).
22. Wade, K. Structural and bonding patterns in cluster chemistry *Adv. Inorg. Chem. Radiochem.* **18,** 1–66 (1976).
23. Longuet-Higgins, H. C. & Roberts, M. de V. The electronic structure of an icosahedron of boron atoms. *Proc. R. Soc. London A* **230,** 110 (1955).
24. Mondal, S. *et al.* Electron deficient and polycenter bonds in the high-pressure γ-B_{28} phase of boron. *Phys. Rev. Lett.* **106,** 215502 (2011).
25. Neaton, J. B. & Ashcroft, N. W. Pairing in dense lithium. *Nature* **400,** 141–144 (1999).
26. Azevedo, L. J., Venturini, E. L., Emin, D. & Wood, C. Magnetic susceptibility study of boron carbides. *Phys. Rev. B* **32,** 7970–7972 (1985).
27. Chauvet, O., Emin, D., Forro, L., Aselage, T. L. & Zuppiroli, L. Spin susceptibility of boron carbides: dissociation of singlet small bipolarons. *Phys. Rev. B* **53,** 14450–14457 (1996).
28. Nonhebel, D. C. & Walton, J. C. *Free-Radical Chemistry: Structure and Mechanism*, Cambridge University Press, London UK (1974).
29. Itoh, T., Nakata, Y., Hirai, K. & Tomioka, H. Triplet diphenylcarbenes protected by trifluoromethyl and bromine groups. A triplet carbene surviving a day in solution at room temperature. *J. Am. Chem. Soc.* **128,** 957–967 (2006).
30. Sabatini, J. J., Poret, J. C. & Broad, R. N. Boron carbide as a barium-free green light emitter and burn-rate modifier in pyrotechnics. *Angew. Chem. Int. Ed.* **50,** 4624–4626 (2011).
31. Reddy, K. M., Liu, P., Hirata, A., Fujita, T. & Chen, M. W. Atomic structure of amorphous shear bands in boron carbide. *Nat. Commun.* **4,** 2483 (2013).
32. An, Q., Goddard, W. A. & Cheng, T. Atomistic Explanation of Shear-Induced Amorphous Band Formation in Boron Carbide. *Phys. Rev. Lett.* **113,** 095501 (2014).
33. Schreurs, A. M. M., Xian, X. & Kroon-Batenburg, L. M. J. EVAL15: a diffraction data integration method based on ab initio predicted profiles. *J. Appl. Crystallogr.* **43,** 70–82 (2010).
34. Volkov, A., Macchi, P., Farrugia, L. J., Gatti, C., Mallinson, P., Richter, T. & Koritsanszky, T. (2006). XD2006, A Computer Program Package for Multipole Refinement, Topological Analysis of Charge Densities and Evaluation of Intermolecular Energies from Experimental or Theoretical Structure Factors. URL http://xd.chem.buffalo.edu/

Acknowledgements

We thank Carsten Paulmann for assistance with the x-ray diffraction experiments at beamline F1 of Hasylab at DESY, Hamburg, Germany. Financial support has been obtained from the German Science Foundation (DFG—"Deutsche Forschungsgemeinschaft") under project No. Sm 55/24-1. N.D. thanks the DFG for financial support through the Heisenberg Program and Project No. DU 954-8/1. N.D. and L.D. gratefully acknowledge the Federal Ministry of Education and Research (BMBF, Germany) for funding.

Author Contributions

S.v.S. planned and coordinated the study. N.D. and G.P. grew the single crystals. S.M., E.B. and L.D. selected the crystal by single-crystal x-ray diffraction. S.M., S.D. and S.I.A. collected diffraction data for the electron-density analysis. S.M. performed the electron-density study. S.v.S. and S.M. wrote the paper. All authors contributed to the discussion.

Additional Information

Supplementary information accompanies this paper at http://www.nature.com/srep

Competing financial interests: The authors declare no competing financial interests.

How to cite this article: Mondal, S. *et al.* Disorder and defects are not intrinsic to boron carbide. *Sci. Rep.* **6**, 19330; doi: 10.1038/srep19330 (2016).